TECHNICAL TRANSACTIONS | CZASOPISMO TECHNICZNE
CIVIL ENGINEERING | BUDOWNICTWO

3-B/2015

IWONA GALMAN*, JAN KUBICA*

STRESS–STRAIN CHARACTERISTICS OF BRICK MASONRY UNDER COMPRESSIVE CYCLIC LOADING

ZALEŻNOŚCI NAPRĘŻENIE – ODKSZTAŁCENIE MURÓW CERAMICZNYCH ŚCISKANYCH CYKLICZNIE

A b s t r a c t

This paper presents the results of laboratory experiments carried out on twelve clay brick masonry wallettes of two types under cyclic compressive loading. In the paper, the procedure adapted for testing is described and the results are discussed. The failure models and cracking patterns of the tested specimens are presented. The effects of the repeated load on the behaviour and mechanical properties of the wall are observed and discussed. Based on the results, the analytical formula for the determination of the failure envelope curve is also proposed.

Keywords: *uniaxial compression tests, brick masonry, cyclic loading, envelope curve*

S t r e s z c z e n i e

W artykule zaprezentowano rezultaty badań laboratoryjnych dwóch serii (łącznie 12) murów poddanych cyklicznej sile ściskającej. Przedstawiono procedury badań i obrazy zniszczenia, a wyniki poddano dyskusji. Obserwowano wpływ powtarzającego sie obciążenia ściskającego na zachowanie i parametry materiałowe muru. Podjęto próbę analitycznego opisu krzywej charakterystycznej: obwiedni.

Słowa kluczowe: *ściskanie, mury ceglane, obciążenie cykliczne, obwiednie badania cyklicznego*

DOI: 10.4467/2353737XCT.15.162.4337

* Ph.D. Iwona Galman, Prof. Jan Kubica, Department of Structural Engineering, Silesian University of Technology.

1. Introduction

Stress–strain relationship σ–ε is taken as the basic characteristic of material behaviour under loading. Usually, it is a curvilinear relationship dependent upon different factors. One of these factors is the loading scheme. Laboratory and theoretical investigations of the σ–ε relationship have been conducted for several years in many research centres worldwide. It is worth mentioning the paper published by Kaushik et al. [1] covering the collection and juxtaposition of test results and analytical considerations on the stress–strain relationship in masonry walls loaded to failure in one cycle. Nowadays, it could be taken that the σ–ε characteristic of masonry walls under monotonically compression is rather well described, whereas the examination of this relationship of masonry under cyclic loading remains incomplete. Karsan & Jersa [2] were the first to propose a description of the σ–ε characteristic of the cyclically loaded material with three characteristic curves: the envelope curve, the stability-point curve and the common-point curve of the σ–ε relationship. These recommendations, although initially developed for concrete, were also adopted for the characterisation of masonry. Since the nineteen-seventies, there have been trials to mathematically describe these curves. Sinha [3−5] proposed a definition of the σ–ε curve with an exponential function. Later, Nazar & Sinha [6] represented the characteristic curves with a fourth-order polynomial function. In 2013, Alshebani [7] returned to exponential representation. Evolution and different approaches to mathematical (analytical) description were also observed in the definition of loading curve (exponential [8], polynomial [9, 10]), which is useful in the assessment of damage intensity of the structure.

Conclusions from these analyses are interesting from a qualitative point of view. Nevertheless, the results have no practical use or quantitative meaning in Poland or other Central European countries as the tests were conducted on different types of masonry than those used in Central Europe. Moreover, results of these investigations were often contradictory to each other. Therefore, it is necessary to perform such analyses with masonry walls made of the most popular local components: solid clay brick on cement–lime mortar.

2. Experimental test

The experimental investigations were performed on two types of test specimens made of solid clay brick of strength class '15' (f_b = 18.7 N/mm^2) and cement–lime mortar (1:1:6) class M5 (f_m = 6.8 N/mm^2). Specimens of **CV** type were used to determine the compressive strength of masonry and the stress-strain relationship according to the method given in EN 1052-1:2001 [11]. Masonry specimens of **MW** type had higher overall dimensions (according to the requirements specified in standard [11]) and the most popular thickness used in the construction of load-bearing walls in Poland (1 brick, i.e. 250 mm). Dutch/Flemish bond (also very popular in Poland) was applied so the longitudinal joint was formed in every second layer.

The shape, dimensions and the view of both types of test specimens ready for testing are shown in Fig. 1.

a)

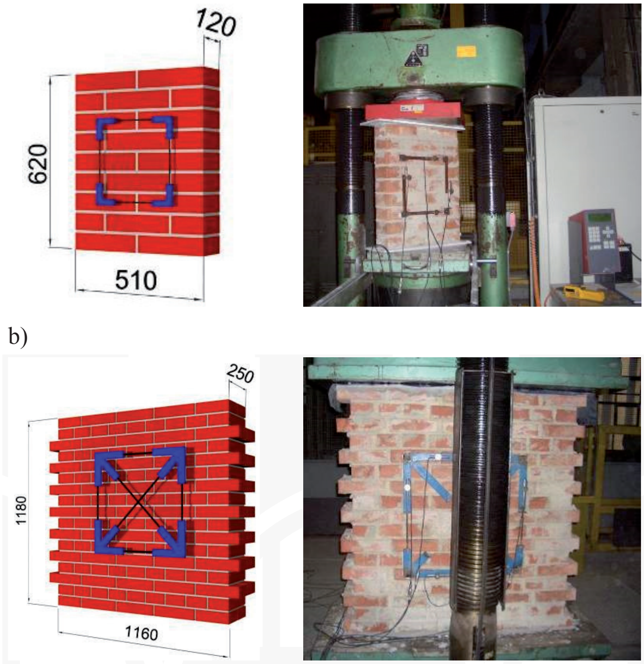

Fig. 1. The shape, dimensions and view of both types of specimens ready for testing: a) type **CV**; b) type **MW**

Measuring frames with inductive (LVDT) sensors for the purposes of measuring deformations to an accuracy of 0.0002 mm were located on both sides of each masonry specimen. The dimensions of a frame, recording vertical and horizontal deformations, were equal to 300 × 300 mm in case of **CV** models and 600 × 600 mm in case of walls **MW**.

The tests of the **CV** type masonry wallettes (smaller specimens) were performed using a hydraulic press machine with a 2000 kN range capacity while the tests of the **MW** masonry walls were carried out using a hydraulic press machine with a maximal range of 6000 kN. Before placing the specimens in the press machine, both top and bottom surfaces of each specimen were levelled with a cement mortar. To eliminate friction between the surfaces of the steel heads of the machine and the specimens' surfaces, special pads were used: 10 mm Teflon pads for the **CV** series specimen and a double layer of polyurethane foil with graphite grease between the layers for the **MW** series specimens.

Three of the six **CV** series specimens and five of the six **MW** series wallettes were cyclically loaded with the load increasing in each cycle. The rest of the specimens were used as reference members and were loaded in one cycle. The loading history for the cyclically compressed masonry is presented in Fig. 2.

The load ratio during all tests was equal to 2 kN/s. The first level of load for the **CV** series masonry specimens was equal to 50 kN and was then increased by 50 kN in each cycle. The first level of load for the **MW** series walls was equal to 300 kN, then 600, 900 and 1200 kN, in the next cycles, this was stepped up by 150 kN until failure. For each cycle, the load was sustained for ~3 minutes in order to stabilise the state of deformations.

a) b)

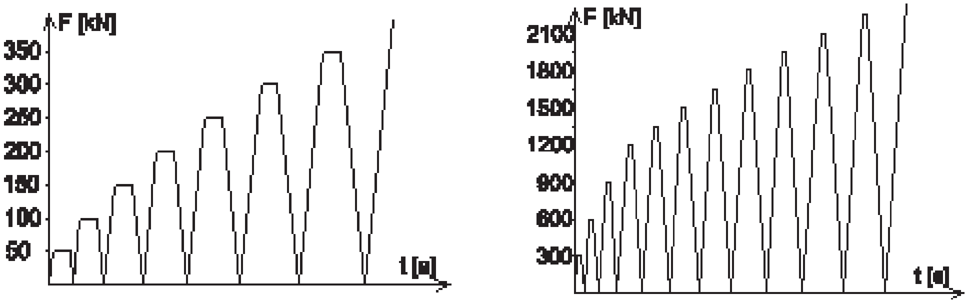

Fig. 2. Loading history for specimen testing: a) **CV** series; b) **MV** series

Table 1

Exemplary failure patterns

Series	One cycle loading		Cyclic loading	
	side A	side B	side A	side B
CV	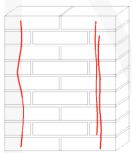	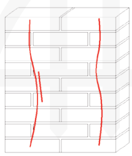	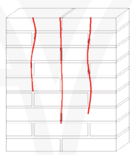	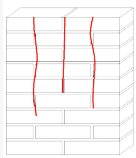
	CV-d-2		CV-c-2	
MW	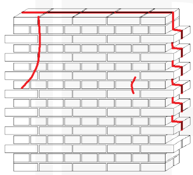	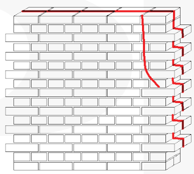	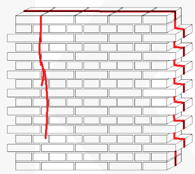	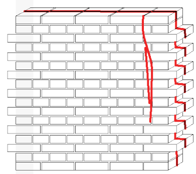
	MW-d		MW-c-1	

3. Test result and discussion

3.1. Modes of failure

Significant differences between modes of failure of specimens loaded cyclically and those loaded in one cycle were not observed. Exemplary sketches of failure (crack) patterns of masonry wallettes representing both series and both types of loading are shown in Table 1. All tested elements (**MW** and **CV** series) failed in a similar manner independent of the mode of loading (cyclic or in one cycle). In Fig. 3, an exemplary failure of **MW** series masonry wallettes as well as the **CV** series are presented.

a) b)

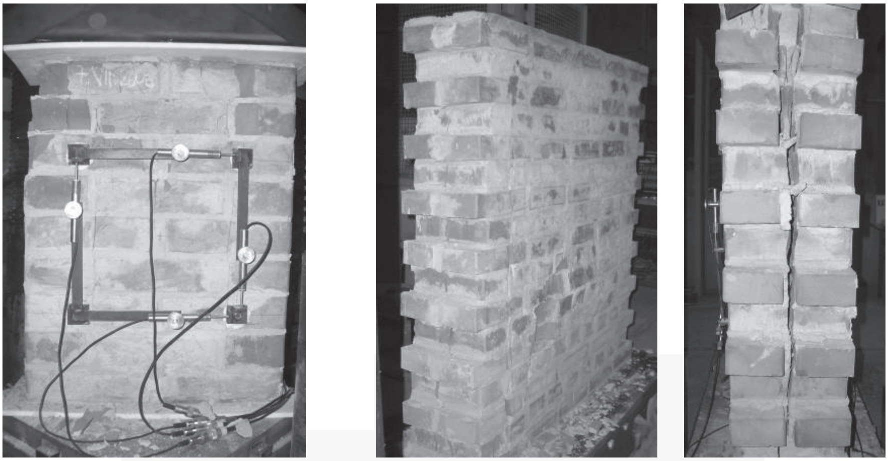

Fig. 3. Failure of: a) **CV** type model; b) **MW** type model

The failure was caused by the formation of a few cracks oriented perpendicularly to the bed joints which divided the specimen into a few independent columns, see Fig. 3. In case of the wallettes with a thickness of one brick (**MW** series), splitting in the plane of a longitudinal joint was additionally observed. The cracking parallel to the face surface of the wall divided the specimen into two independent wall plates as is shown in Fig. 3b.

3.2. Main results

The main results of the investigations, which include cracking stresses σ_{cr} (corresponding to the first crack appearance), ultimate stresses σ_u and corresponding strains ε_{cr} and ε_u, are presented in Table 2. The average values of strains ε_{cr} and ε_u were determined based on the data recorded by four LVDT sensors. In the sixth column of Table 2, the correlation between σ_{cr} and σ_u stresses is shown. The last column displays the number of cycles at which the point of failure war reached for each tested specimens (including reference members loaded in one cycle).

The first cracks in the small specimens with thicknesses of 1/2 of a brick (**CV** type) appeared at the σ_{cr} stress level of 6.52–7.34 N/mm^2. The value of the ultimate stress at failure for these panels was similar and ranged from 11.85 to 14.92 N/mm^2. An increase in the cracking strain ε_{cr} and ultimate strain ε_u of the cyclically loaded wall with respect to elements loaded in one cycle was observed (by 9% and 17% respectively).

In larger walls (**MW** series), the first cracks in cyclically loaded elements appeared at the stress level of 4.78–6.15 N/mm^2, while in monotonically loaded wallettes the first cracks were observed at a slightly higher level of stress, 6.38 N/mm^2. The value of the ultimate stress at failure was similar for all tested specimens of this type and ranged between 8.67 and 10.71 N/mm^2. Analogically to the elements in the **CV** series, it was observed that the ratio between the cracking stress, σ_{cr}, and the ultimate stress, σ_u, was quite similar. The value of the ultimate strain in the wallette loaded in one cycle was only slightly smaller than in the specimens subjected to cyclic loading.

The number of cycles was similar for all masonry walls subjected to repeating load. It seems that shape and overall dimensions as well as the existence of longitudinal joints at every second level, as in the case of **MW** series specimens, have no influence on the number of cycles required to reach the point of failure for masonry wallettes subjected to uniaxial compression.

Table 2

Main results of investigations

Test specimen	σ_{cr} [N/mm²]	σ_u [N/mm²]	ε_{cr} [ε_u 10^{-3}]	ε_u [$\times 10^{-3}$]	σ_{cr}/σ_u	Number of cycles
CV-d-1	6.83	13.14	0.92	2.61	0.52	1
CV-d-2	7.31	14.92	0.94	2.54	0.49	1
CV-d-3	6.98	13.98	1.02	2.63	0.50	1
CV-c-1	6.52	12.48	0.94	2.89	0.52	16
CV-c-2	7.34	14.57	1.04	3.29	0.50	18
CV-c-3	7.11	11.85	1.16	2.91	0.60	15
MW-d	6.38	10.42	1.03	2.35	0.61	1
MW-c-1	5.55	9.94	0.90	2.5	0.56	15
MW-c-2	5.48	9.36	1.01	2.65	0.59	14
MW-c-3	6.15	10.71	0.93	2.47	0.53	16
MW-c-4	4.78	8.67	0.77	2.45	0.55	13
MW-c-5	5.96	9.89	0.97	2.71	0.60	15

3.3. Failure envelope

The results of cyclic tests allowed defining a failure envelope of the stress–strain relationship. The envelope is created by connecting points of the maximum strain in each cycle. A typical σ–ε relationship for masonry subjected to cyclic loading with the envelope is presented in Fig. 4.

To eliminate the material and strength differences, further comparison of results was performed with normalized $\sigma_i/\sigma_{\max,i} - \varepsilon_i/\varepsilon(\sigma_{\max})$ relationships. Averaged normalised failure envelopes for the **CV** and **MW** masonry walls are shown below in Fig. 5.

It was observed that in the high initial range of compressive stresses (up to ~0.7 $\sigma_{\max}$) for masonry with a half-brick thickness (**CV** series), the resultant relationships are linear which signifies near-elastic behaviour of the masonry. For specimens with a thickness of 1 brick (**MW** series) up to a level of ~30% of $\sigma_{\max}$ (first visible crack appearance), the diagrams have a distinctly curvilinear character (non-linear elastic behaviour of the material) and then, in the range from 30% to ~75% of $\sigma_{\max}$ (rapidly increasing plastic-brittle damage deformations), fracture development stabilises at the similar level and the diagrams have a more or less

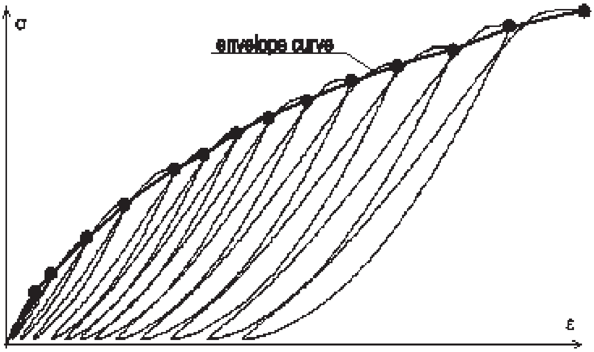

Fig. 4. Typical σ–ε relationship for masonry subjected to cyclic loading with the construction of the envelope curve

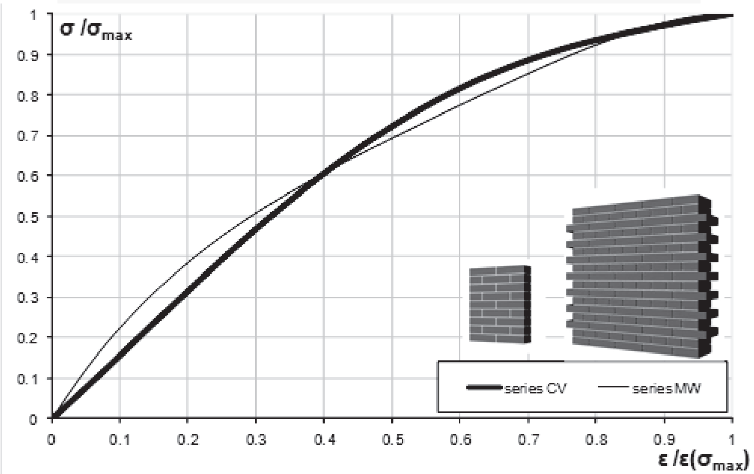

Fig. 5. Averaged normalised envelopes for **MW** and **CV** series models

linear character. This can be explained by the fact that in the **MW** series masonry walls, there is an unbounded longitudinal joint located at every second layer in the axis of the wall which has an effect on the behaviour of that wall. When stresses exceed the value of 75% of σ_{max}, the process of fracture and disintegration of the material is very quick, leading to failure.

Describing the curves with fourth-order polynomials, the following proposed formula was used:

$$\frac{\sigma}{\sigma_{max}} = a \cdot \left(\frac{\varepsilon}{\varepsilon(\sigma_{max})} \right)^4 + b \cdot \left(\frac{\varepsilon}{\varepsilon(\sigma_{max})} \right)^3 + c \cdot \left(\frac{\varepsilon}{\varepsilon(\sigma_{max})} \right)^2 + d \cdot \frac{\varepsilon}{\varepsilon(\sigma_{max})} \quad (1)$$

where *a*, *b*, *c*, *d* are polynomial coefficients (determined values are specified in Table 3).

Table 3

Constant coefficients of **polynomial function**
$\boldsymbol{\sigma/\sigma_{max,i} - \varepsilon/\varepsilon(\sigma_{max,i})}$ for eq. (1)

Series	Values of constant coefficients			
	a	*b*	*c*	*d*
MW	–2.17	5.00	–4.47	2.64
CV	1.16	–2.52	0.87	1.49

The next diagram (Fig. 6) presents $_i/\sigma_{max,i} - \varepsilon_i/\varepsilon(\sigma_{max,i})$ relationship for the one cycle tests (continuous line) and the failure envelope obtained from the cyclic tests (dashed line) for the **CV** and **MW** masonry walls series.

a) b)

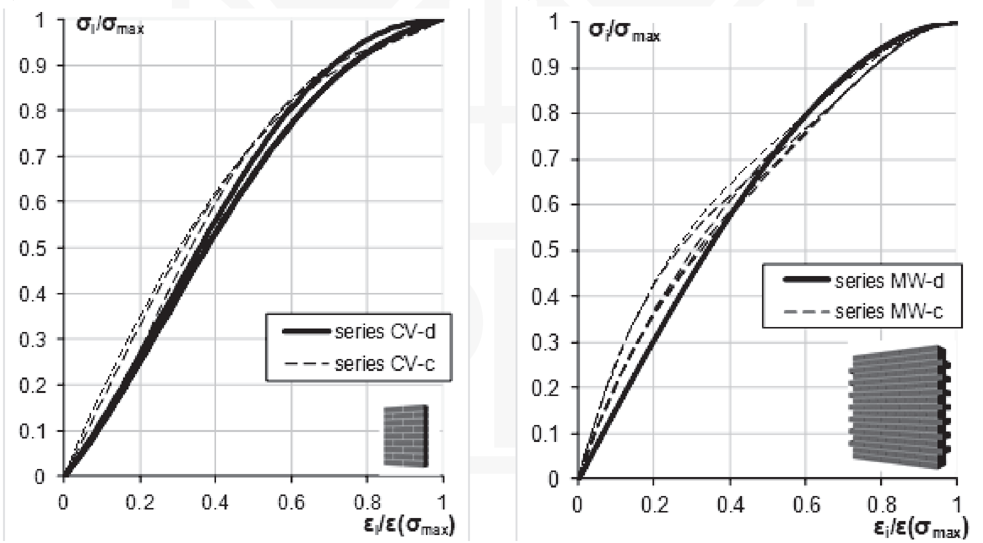

Fig. 6. Normalised $\sigma_i/\sigma_{max,i} - \varepsilon_i/\varepsilon(\sigma_{max,i})$ relationships for: a) **CV**, b) **MW** series models

It was observed that the characteristic obtained from the monotonic tests, both for the **CV** and **MW** series elements, differs significantly from the envelope of the cyclically loaded elements – it has a linear characteristic over a greater range than in the case of monotonically loaded masonry walls. The curves obtained in the cyclic tests show that at the level of ~30% of the ultimate stress softening or even local depletion of load-bearing capacity is observed in the areas where brittle fracture occurred. In the subsequent cycles, non-elastic strains develop.

3.4. Loading curves

Knowledge of σ–ε loading curves in cyclic compressive loading allows evaluating the damage intensity of the structures. Exemplary σ–ε relationship for the loading curves of the masonry walls with a one-brick thickness (**MW-c-1**) is shown in Fig. 7. The dashed line corresponds to the cycle when the first cracks were appeared. Based on this figure, the value of strains related to cracking stresses σ_{cr} (values given in column 2 of Table 2) is ε_{cr} (values shown in column 4 of Table 2). After unloading, the residual value of strain amounted to $\varepsilon_{cr,r}$. In the following loading cycles the value of residual strains clearly increased while the values of initial modulus of elasticity (tangent of the angle of stress-strain relationship $E_i = (\Delta\sigma_i/\Delta\varepsilon_i)$, determined for each cycle from the stress range 0 to $1/3\sigma_{\max,i}$) decreased systematically.

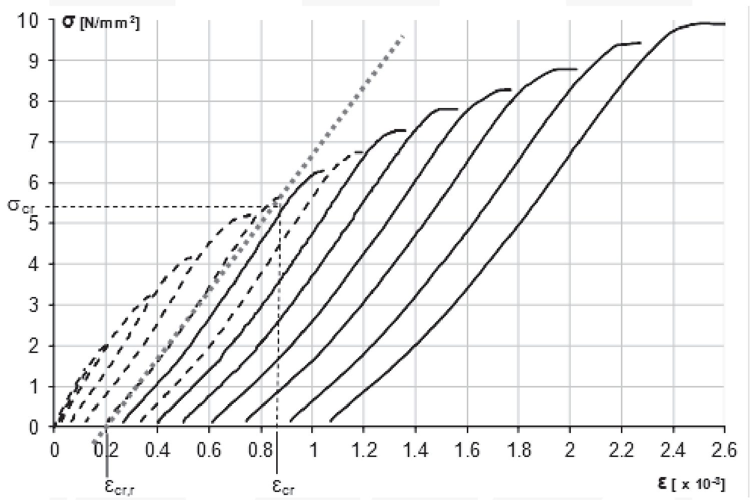

Fig. 7. Normalised $\sigma_i/\sigma_{\max,i} - \varepsilon_i/\varepsilon(\sigma_{\max,i})$ relationships for: a) **CV**, b) **MW** series models

The shape of the loading curves for the **MW** series changes with the developing degradation of the masonry walls. The curves before cracking have different characteristics that the curves after cracking. The phenomenon of the curvature change during the process of cyclic loading was not observed in the masonry walls with half-brick thickness.

Graphical interpretation of the normalised loading curves for both types of tested specimens is presented in Fig. 8.

The loading curve for the **MW** masonry walls before cracking clearly has a linear-elastic character whereas the loading curve after cracking is a concave curve. In the cracked material, relaxation is observed when the element is unloaded. During the following loading cycle, firstly, the existing damage is compressed and the cracks are closed. The change of the curve from concave to convex is observed if such material starts to behave as new, undamaged material. A hardening effect is then observed. This phenomenon was observed only in the case of **MW** series wallettes. It is probably also connected with the existence of an internal longitudinal crack at every second level of the wallette. Horizontal tensile stresses in a direction perpendicular to the plane of the specimen produced by vertical compressive loads generated the internal cracks and local damage. Therefore, the degradation process is more distinct.

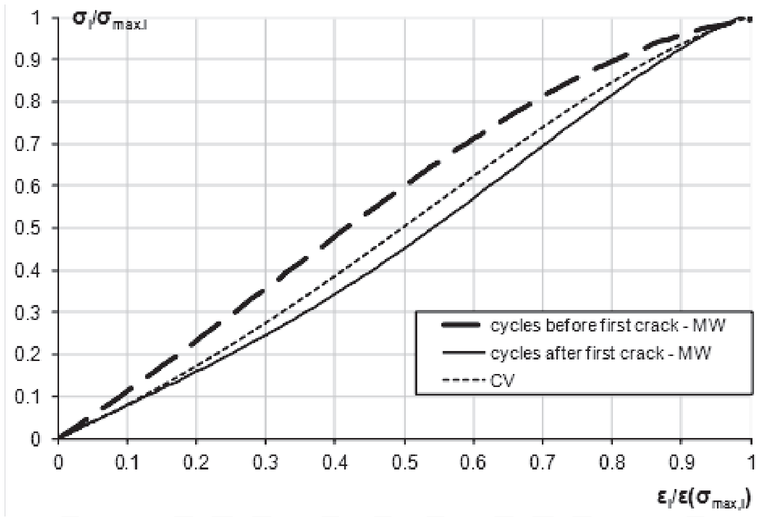

Fig. 8. Normalised loading curve $\sigma_i/\sigma_{max,i} - \varepsilon_i/\varepsilon(\sigma_{max,i})$

There was no need to group the loading curves into curves before and after cracking for the half-brick thick masonry wallettes (**CV** series); σ–ε loading curve was well described for all cycles by a single relationship. Graphically, the loading curve for the **CV** series lies between the curves for the **MW** series. Its shape is close to linear – strains increase proportionally to stresses.

3.5. Discussion of results

Figure 9 presents a comparison of envelope curves of cyclic tests performed by the authors and the relationships obtained by other authors.

Differences between the presented curves can be observed. These differences are due to the use of different materials for construction of the wallettes as well as different dimensions of the testing elements.

Obviously, the wallettes made with the use of wedging elements (as was the case in external research examples) will exhibit a higher load-bearing capacity than the wallettes made from bricks without a mechanical wedge. The envelope curves obtained in the tests of the wallettes with small-size self-wedging elements are located above the analogical curves obtained for the full-brick wallettes.

Moreover, as was the case in the **MW** series wallettes, the use of the longitudinal joint significantly weakens the wallette. Lower values of stresses cause higher strains in comparison to the wallettes without an internal joint.

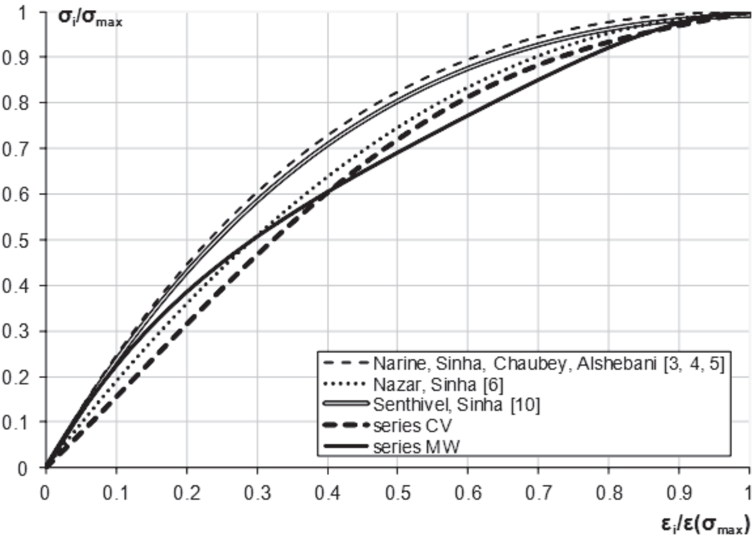

Fig. 9. Normalised $\sigma_i/\sigma_{max,i} - \varepsilon_i/\varepsilon(\sigma_{max,i})$ relationships for own and external research

In general, based on the presented diagram it can be stated that the cyclic-load envelope curve has two forms: before cracking and after cracking. Before cracking, its course is more linear (except for the **MW** series, which was discussed in 3.3). After reaching cracking stress level, a change of curvature can be observed due to the degradation of the wallette caused by cracking and damage.

5. Summary and conclusions

The paper presents the results of laboratory tests of 12 masonry wallettes subjected to compressive loading. The walls differed in shape, overall dimensions and loading scheme. Based on the results of the presented tests and analytical analyses, the following conclusions may be formulated:
- the values of the cracking strain, ε_{cr}, and the ultimate strain, ε_u, of cyclically loaded masonry walls are greater than the values obtained for monotonic loading tests;
- the values of the cracking stresses, σ_{cr}, and the ultimate stresses at failure, σ_u, do not depend on the loading scheme;
- σ–ε relationship for masonry wallettes loaded in one cycle is different than the envelope obtained in cyclic loading: the character of the envelope of σ–ε curves for the cyclically loaded elements is considerably more non-linear than the character of this envelope for the monotonically loaded elements;
- the characteristic of the σ–ε loading curve allows describing the evaluation of damage intensity of the structure;

– in the case of masonry walls with an internal joint (**MW** series), the shape of the loading curve changes due to the progressive degradation of masonry during cyclic loading;
– the proposed mathematical description of the envelope curve does not have a universal character due to the limited number of tested specimens and using only one type of masonry units and mortar, further investigations, both experimental and analytical are necessary.

References

[1] Kaushik H., Rai D., Jain S., *Stress-Strain Characteristics of Clay Brick Masonry under Uniaxial Compression*, Journal of Materials in Civil Engineering, ASCE, Vol. 19, No. 9, 2007, 728–739.

[2] Karsan J., Jersa J., *Behavior of Concrete Under Compressive Loading*, Journal of Structural Division, ASCE, Vol. 95, No. 12, 1969, 2543–2563.

[3] Naraie K., Sinha S., *Behaviour of Brick Masonry Under Cyclic Compressive Loading*, Journal of Construction Engineering and Management, 1989, 1432–1445.

[4] Chaubey U., Sinha S., *Cyclic compressive loading response of brick masonry*, Journal of Masonry International, Vol. 4, No. 3, 1991, 94–98.

[5] Alshebani M., Sinha S., *Stress- Strain Characteristics of Brick Masonry Under Uniaxial Cyclic Loading*, Journal of Structural Engineering, Vol. 125, No. 6, 1999, 600–604.

[6] Nazar M., Sinha S., *Mathematical model for loading/unloading stress-strain curves of interlocking brick masonry*, Proc. 7th International Masonry Conference, London 2006.

[7] Alshebani M., *Permissible Stress Level of Brick Masonry under Compressive Cyclic Loading*, Journal of Civil Engineering and Architecture, Vol. 7, 2013, 153–157.

[8] Narin K., Sinha S., *Loading and Unloading Stress-Strain Curves for Brick Masonry*, Journal of Structural Engineering, 1989, 2631–2644.

[9] Alshebani M, Sinha S., C*yclic compressive loading unloading curves of brick masonry*, Structural Engineering and Mechanics, 1999, 375–382.

[10] Senthivel R., Sinha S., *Behaviour of Calcium Silicate Brick Masonry Under Cyclic Uniaxial Compression. Masonry*, Proc. 6th International Masonry Conference, Vol. 9, London 2002, 412–422.

[11] EN 1052-1:2001 Methods of test for Masonry – Part 1:Determination of compressive strength.